Syntheses, Structures, Magnetic Properties, and X-ray Absorption Spectra of Carnotite-type Uranyl Chromium(V) Oxides: $A[(UO_2)_2Cr_2O_8](H_2O)_n$ ($A = K_2$, Rb_2, Cs_2, Mg; $n = 0$, 4)

A. J. Locock,*,† S. Skanthakumar,‡ P. C. Burns,† and L. Soderholm‡

Department of Civil Engineering and Geological Sciences, University of Notre Dame, 156 Fitzpatrick Hall, Notre Dame, Indiana 46556, and Chemistry Division, Argonne National Laboratory, 9700 South Cass Avenue, Argonne, Illinois 60439

Received November 11, 2003. Revised Manuscript Received February 2, 2004

Four uranyl chromium(V) oxides were synthesized by mild hydrothermal methods and their structures were solved using single-crystal X-ray diffraction data. In these structures, U occurs in edge-sharing dimers of UO_7 uranyl pentagonal bipyramids, and Cr occurs in edge-sharing dimers of CrO_5 square pyramids. The two sets of dimers share edges, forming sheets of composition $[(UO_2)_2Cr_2O_8]^{2-}$ that are topologically identical to uranyl divanadate sheets, $[(UO_2)_2V_2O_8]^{2-}$, that occur in compounds of the carnotite group. $K_2[(UO_2)_2Cr_2O_8]$ (**KUCr**), $Rb_2[(UO_2)_2Cr_2O_8]$ (**RbUCr**), and $Cs_2[(UO_2)_2Cr_2O_8]$ (**CsUCr**) are isostructural with $K_2[(UO_2)_2V_2O_8]$, and $Mg[(UO_2)_2Cr_2O_8](H_2O)_4$ (**MgUCr**) is isostructural with $Ni[(UO_2)_2V_2O_8](H_2O)_4$. The stoichiometries of these compounds imply that Cr is present as chromium(V), which is supported by the results of bond valence analyses. EPR spectra and magnetic susceptibility data for **KUCr** are consistent with the presence of the d^1 cation chromium(V). The **KUCr** moments undergo a sharp transition from paramagnetic to antiferromagnetic behavior at $T_N = 18.5$ K. XAFS data for the U L_3 edge and XANES of the Cr K edge of **KUCr** yield coordinations and oxidation states consistent with the crystal structure analysis. The presence of a pre-edge peak due solely to Cr^{5+} sounds a cautionary note for XANES determination of the chromate(VI) content of environmental samples. Crystallographic data for **KUCr**, **RbUCr**, **CsUCr**: monoclinic space group $P2_1/c$ (No. 14), with $a = 6.5483(8)$ Å, $b = 8.3548(10)$ Å, $c = 10.4200(13)$ Å, $\beta = 105.040(3)°$; $a = 6.8677(6)$ Å, $b = 8.3599(7)$ Å, $c = 10.4625(8)$ Å, $\beta = 106.004(2)°$; and $a = 7.2643(15)$ Å, $b = 8.3803(17)$ Å, $c = 10.5100(22)$ Å, $\beta = 106.399(5)°$, respectively. Crystal data for **MgUCr**: orthorhombic space group *Pnma* (No. 62), with $a = 10.5825(19)$ Å, $b = 15.1337(27)$ Å, $c = 8.1425(14)$ Å.

Introduction

Chromium(V) is an uncommon oxidation state most often observed in solution (via EPR) as a transient species in the course of the reduction of chromium(VI) to chromium(III).[1] However, Cr^{5+} is of considerable interest in the environmental chemistry and biochemistry of chromium, because of its importance in understanding the carcinogenic mechanisms of chromate(VI).[2−4] Although most solutions of Cr^{5+} are unstable and rapidly disproportionate to Cr^{6+} and Cr^{3+}, there are a number of chromium(V)−organic complexes, several of which have substantial lifetimes in biologic systems.[3,5−8] The chromium(V) in these complexes is frequently present in square pyramidal coordination with oxygen: $CrO(O_4)$.[3,5−8] In contrast, in solid oxides, the discrete tetrahedral chromate(V) ion, CrO_4^{3-}, is the most common coordination state.[1] The alkali chromates(V) are hygroscopic, whereas the alkaline earth chromates(V) and lanthanide chromates(V) are stable under ambient conditions.[1,9−13] The chemistry of Cr^{5+} has been reviewed in considerable detail.[1,13−15]

* Corresponding author. E-mail: alocock@nd.edu.
† University of Notre Dame.
‡ Argonne National Laboratory.

(1) Cotton, F. A.; Wilkinson, G.; Murillo, C. A.; Bochmann, M. *Advanced Inorganic Chemistry*; John Wiley & Sons: New York, 1999; pp 737−756.
(2) Sakurai, H.; Takechi, K.; Tsuboi, H.; Yasui, H. *J. Inorg. Biochem.* **1999**, *76*, 71−80.
(3) Farrell, R. P.; Lay, P. A. *Comments Inorg. Chem.* **1992**, *13*, 133−175.
(4) Connett, P. H.; Wetterhahn, K. E. *Struct. Bonding (Berlin)* **1983**, *54*, 93−124.
(5) Branca, M.; Micera, G.; Segre, U.; Dessi, A. *Inorg. Chem.* **1992**, *31*, 2404−2408.
(6) Bramley, R.; Ji, J.-Y.; Lay, P. A. *Inorg. Chem.* **1991**, *30*, 1557−1564.
(7) Nishino, H.; Kochi, J. K. *Inorg. Chim. Acta* **1990**, *174*, 93−102.
(8) Bramley, R.; Ji, J.-Y.; Judd, R. J.; Lay, P. A. *Inorg. Chem.* **1990**, *29*, 3089−3094.
(9) Jiménez, E.; Isasi, J.; Sáez-Puche, R. *J. Solid State Chem.* **2002**, *164*, 313−319.
(10) Jiménez, E.; Isasi, J.; Sáez-Puche, R. *J. Alloys Compd.* **2001**, *323−324*, 115−118.
(11) Aoki, Y.; Konno, H. *J. Solid State Chem.* **2001**, *156*, 370−378.
(12) Jiménez, E.; Isasi, J.; Sáez-Puche, R. *J. Alloys Compd.* **2000**, *312*, 53−59.
(13) Mitewa, M.; Bontchev, P. R.*Coord. Chem. Rev.* **1985**, *61*, 241−272.
(14) Nag, K.; Bose, S. N.*Struct. Bonding (Berlin)* **1985**, *63*, 154−197.

10.1021/cm030639c CCC: $27.50
Published on Web 03/09/2004

Uranyl compounds and minerals have also received attention recently, owing to their importance to the environment[16] and to their extraordinary chemical and structural complexity.[17,18] They are important for understanding the genesis of the oxidized portions of U deposits and water−rock interactions in such deposits, and are common in mine and mill wastes generated as byproducts of the utilization of U resources.[19] They form in uranium-contaminated soils[19] and are expected to be abundant alteration products of nuclear wastes stored under conditions similar to those expected in the proposed repository at Yucca Mountain[20,21] and may impact significantly upon the release of radionuclides in such systems.[22−25] Uranyl compounds possess a range of physicochemical properties that provide for technological uses, and recent studies have focused on the synthesis of a range of inorganic and mixed organic−inorganic uranyl compounds.[26−29]

Uranyl compounds of chromium are dominated by the chromate(VI) anion, CrO_4^{2-}; at least 28 inorganic uranyl chromates are listed in the International Centre for Diffraction Data's Powder Diffraction File. However, structure refinements have been published only for a few inorganic uranyl chromates[30−34] and several hybrid organic−inorganic uranyl chromates,[35−42] although this is an area of current interest.[43] As part of our ongoing research into the solid-state chemistry of uranyl structures, we have synthesized four uranyl chromium(V) compounds, characterized their structures, and used their magnetic properties to confirm the presence of Cr^{5+}. To our knowledge, these are the first actinide compounds of pentavalent chromium.

Materials and Methods

Caution: Chromium(VI) compounds are carcinogenic, and chromium(V) compounds are mutagenic and potentially carcinogenic, and their handling requires extra care. Although all uranium materials used in these experiments were isotopically depleted, standard precautions for handling radioactive materials should be followed.

Synthesis. $Na_2Cr_2O_7(H_2O)_2$ (99.8%, Fisher), $K_2Cr_2O_7$ (99.9%, Fisher), $NaNO_3$ (99.2%, Fisher), $RbNO_3$ (99%, Alfa Aesar), $CsNO_3$ (99.8%, Alfa Aesar), and $UO_2(NO_3)_2(H_2O)_6$ (98%, Alfa Aesar) were used as received. $Mg(NO_3)_2(H_2O)_6$ was prepared from MgO (98%, Fisher) and concentrated $HNO_{3(aq)}$ (69.2%, Fisher). Millipore-filtered ultrapure water (18 MΩ resistance) was used in all reactions. Reactions were carried out in 23 mL poly(tetrafluoroethylene)-lined Parr acid-reaction vessels. Reaction yields were low (<25% on a uranium basis) and were not quantitatively determined because of the presence of other phases.

$K_2[(UO_2)_2Cr_2O_8]$. **KUCr** was synthesized by hydrothermal reaction of $UO_2(NO_3)_2(H_2O)_6$ (134.4 mg, 0.2677 mmol), $NaNO_3$ (338.7 mg, 3.985 mmol), $K_2Cr_2O_7$ (124.7 mg, 0.4239 mmol), and ultrapure H_2O (3390 mg). The mixture was heated at 230(1) °C in a Fisher Isotemp oven for 24 days. The autoclave was then removed to air and allowed to cool to room temperature. The solid products consisted of **KUCr** and minor α-CrOOH (grimaldiite structure) and were filtered, washed with ultrapure water, and air-dried. Interestingly, similar experiments using KNO_3, rather than $NaNO_3$, did not yield **KUCr** crystals of adequate size for study. Use of $LiNO_3$ gave results very similar to those achieved with $NaNO_3$–good quality crystals of **KUCr**. Neither Na nor Li were incorporated into the solid phase. The reason for the presence of reduced cations under the mild hydrothermal conditions used for the syntheses is not immediately apparent. Speciation data for aqueous Cr under elevated temperatures and pressures are not available. The poly(tetrafluoroethylene) liners do not appear to participate in the reactions and no obvious reducing agent is present.

$Rb_2[(UO_2)_2Cr_2O_8]$. **RbUCr** was synthesized by hydrothermal reaction of $UO_2(NO_3)_2(H_2O)_6$ (106.9 mg, 0.2129 mmol), $RbNO_3$ (223.4 mg, 1.515 mmol), $NaCr_2O_7(H_2O)_2$ (157.1 mg, 0.5272 mmol), and ultrapure H_2O (5250 mg). The mixture was heated at 6°/h from 50 to 220(1) °C, held at temperature for 24 h, and cooled to 90(1) °C at 6°/h. The autoclave was then removed to air and allowed to cool to room temperature. The solid products consisted mostly of **RbUCr**, with a trace α-CrOOH, and were filtered, washed with ultrapure water, and air-dried.

$Cs_2[(UO_2)_2Cr_2O_8]$. **CsUCr** was synthesized by hydrothermal reaction of $UO_2(NO_3)_2(H_2O)_6$ (108.7 mg, 0.2165 mmol), $CsNO_3$ (149.3 mg, 0.7660 mmol), $NaCr_2O_7(H_2O)_2$ (115.2 mg, 0.3866 mmol), and ultrapure H_2O (6430 mg). The mixture was heated at 6°/h from 50 to 220(1) °C, held at temperature for 24 h, and cooled to 90(1) °C at 6°/h. The autoclave was then removed to air and allowed to cool to room temperature. The solid products consisted of **CsUCr** and $Cs_2Cr_2O_7$ in an undetermined proportion and were filtered, washed with ultrapure water, and air-dried.

$Mg[(UO_2)_2Cr_2O_8](H_2O)_4$. **MgUCr** was synthesized by hydrothermal reaction of $UO_2(NO_3)_2(H_2O)_6$ (115.0 mg, 0.2290 mmol), $Mg(NO_3)_2(H_2O)_6$ (1052.7 mg, 4.106 mmol), $NaCr_2O_7(H_2O)_2$

(15) Nakagawa, K.; Candelaria, M. B.; Chik, W. W. C.; Eaton, S. S.; Eaton, G. R. *J. Magn. Reson.* **1992**, *98*, 81−91.
(16) Burns, P. C.; Finch, R. J. *Rev. Mineral.* **1999**, *38*.
(17) Burns, P. C.; Miller, M. L.; Ewing, R. C. *Can. Mineral.* **1996**, *34*, 845−880.
(18) Burns, P. C. *Rev. Mineral.* **1999**, *38*, 23−90.
(19) Finch, R. J.; Murakami, T. *Rev. Mineral.* **1999**, *38*, 91−179.
(20) Finn, P. A.; Hoh, J. C.; Wolf, S. F.; Slater, S. A.; Bates, J. K. *Radiochim. Acta* **1996**, *74*, 65−71.
(21) Finch, R. J.; Buck, E. C.; Finn, P. A.; Bates, J. K. *Mater. Res. Soc. Symp. Proc.* **1999**, *556*, 431−438.
(22) Burns, P. C.; Ewing, R. C.; Miller, M. L. *J. Nucl. Mater.* **1997**, *245*, 1−9.
(23) Chen, F.; Burns, P. C.; Ewing, R. C. *J. Nucl. Mater.* **1999**, *275*, 81−94.
(24) Chen, F.; Burns, P. C.; Ewing, R. C. *J. Nucl. Mater.* **2000**, *278*, 225−232.
(25) Burns, P. C.; Olson, R. A.; Finch, R. J.; Hanchar, J. M.; Thibault, Y. *J. Nucl. Mater.* **2000**, *278*, 290−300.
(26) Francis, R. J.; Drewitt, M. J.; Halasyamani, P. S.; Ranganathachar, C.; O'Hare, D.; Clegg, W.; Teat, S. J. *Chem. Commun.* **1998**, *2*, 279−280.
(27) Bean, A. C.; Peper, S. M.; Albrecht-Schmitt, T. E. *Chem. Mater.* **2001**, *13*, 1266−1272.
(28) Bean, A. C.; Albrecht-Schmitt, T. E. *J. Solid State Chem.* **2001**, *161*, 416−423.
(29) Cahill, C. L.; Burns, P. C. *Inorg. Chem.* **2001**, *40*, 1347−1351.
(30) Sykora, R. E.; McDaniel, S. M.; Wells, D. M.; Albrecht-Schmitt, T. E. *Inorg. Chem.* **2002**, *41*, 5126−5132.
(31) Sykora, R. E.; Wells, D. M.; Albrecht-Schmitt, T. E. *Inorg. Chem.* **2002**, *41*, 2304−2306.
(32) Serezhkina, L. B.; Trunov, V. K.; Kholodkovskaya, L. N.; Kuchumova, N. V. *Koord. Khim.* **1990**, *16*, 1288−1291.
(33) Serezhkin, V. N.; Boiko, N. V.; Trunov, V. K. *Zh. Strukt. Khim.* **1982**, *23*, 121−124.
(34) Serezhkin, V. N.; Trunov, V. K. *Kristallografiya* **1981**, *26*, 301−304.
(35) Mikhailov, Yu. N.; Gorbunova, Yu. E.; Demchenko, E. A.; Serezhkina, L. B.; Serezhkina, V. N. *Zh. Neorg. Khim.* **1999**, *44*, 1444−1447.
(36) Mikhailov, Yu. N.; Gorbunova, Yu. E.; Demchenko, E. A.; Serezhkina, L. B.; Serezhkin, V. N. *Zh. Neorg. Khim.* **1998**, *43*, 1831−1833.
(37) Mikhailov, Yu. N.; Gorbunova, Yu. E.; Demchenko, E. A.; Serezhkina, L. B.; Serezhkin, V. N. *Zh. Neorg. Khim.* **1998**, *43*, 971−975.
(38) Mikhailov, Yu. N.; Gorbunova, Yu. E.; Demchenko, E. A.; Serezhkina, L. B.; Serezhkin, V. N. *Dokl. Akad. Nauk* **1998**, *358*, 360−363.
(39) Mikhailov, Yu. N.; Gorbunova, Yu. E.; Serezhkina, L. B.; Serezhkin, V. N. *Zh. Neorg. Khim.* **1997**, *42*, 734−738.
(40) Blatov, V. A.; Strezhkina, L. B.; Serezhkin, V. N. *Koord. Khim.* **1991**, *17*, 1005−1008.
(41) Serezhkin, V. N.; Soldatkina, M. A.; Efremov, V. A.; Trunov, V. K. *Koord. Khim.* **1981**, *7*, 629−633.
(42) Mikhailov, Yu. N.; Orlova, I. M.; Podnebesnova, G. V.; Kuznetsov, V. G.; Shchelokov, R. N. *Koord. Khim.* **1976**, *2*, 1681−1683.
(43) Krivovichev S. V.; Burns P. C. *Z. Krist.* **2003**, submitted.

Table 1. Crystallographic Data and Details of the Structure Refinements

compound	$K_2[(UO_2)_2Cr_2O_8]$	$Rb_2[(UO_2)_2Cr_2O_8]$	$Cs_2[(UO_2)_2Cr_2O_8]$	$Mg[(UO_2)_2Cr_2O_8](H_2O)_4$
a (Å)	6.5483(8)	6.8677(6)	7.2643(15)	10.5825(19)
b (Å)	8.3548(10)	8.3599(7)	8.3803(17)	15.1337(27)
c (Å)	10.4200(13)	10.4625(8)	10.5100(22)	8.1425(14)
b (deg)	105.040(3)	106.004(2)	106.399(5)	90
V (Å^3)	550.6(1)	577.4(1)	613.8(1)	1304.0(1)
space group, Z	$P2_1/c$, 2	$P2_1/c$, 2	$P2_1/c$, 2	$Pnma$, 4
μ Mo Kα (mm^{-1})	32.06	38.22	33.92	26.52
D_{calc} (g/mL)	5.129(1)	5.424(1)	5.616(1)	4.423(1)
crystal size (mm)	0.10 × 0.10 × 0.04	0.08 × 0.06 × 0.01	0.06 × 0.06 × 0.01	0.04 × 0.04 × 0.005
color and habit	dark red plate	dark red plate	dark red plate	dark red plate
θ range of data collection	3.17°−34.52°	3.09°−34.55°	3.16°−34.44°	2.69°−34.49°
total reflections	10988	10469	5478	24508
unique reflections, R_{int}	2296, 0.039	2409, 0.069	2397, 0.148	2819, 0.201
unique $\|F_o\| \geq 4\sigma F$	2056	1760	1015	1025
parameters varied	83	82	52	96
R1[a] for $\|F_o\| \geq 4\sigma F$	2.0	3.0	5.7	5.1
wR2[b] all data	4.3	5.6	11.0	13.3
max. min. peaks (e/Å^3)	3.1, −1.3	5.1, −1.5	2.7, −3.7	7.0, −4.7
isostructural vanadate, reference	$K_2[(UO_2)_2V_2O_8]$[44]	$Rb_2[(UO_2)_2V_2O_8]$[45]	$Cs_2[(UO_2)_2V_2O_8]$[46]	$Ni[(UO_2)_2V_2O_8](H_2O)_4$[47]

[a] $R1 = [\sum||F_o| - |F_c||]/\sum|F_o| \times 100$. [b] $wR2 = [\sum[w(F_o^2 - F_c^2)^2]/\sum(F_o^2)^2]]^{0.5} \times 100$, $w = 1/(\sigma^2(F_o^2) + (aP)^2$, and $P = {}^1/_3[\max(0,F_o^2)] + {}^2/_3F_c^2$.

(135.9 mg, 0.4560 mmol), and ultrapure H_2O (2990 mg). The mixture was heated at 230(1) °C in a Fisher Isotemp oven for 16 days. The autoclave was then removed to air and allowed to cool to room temperature. The solid product consisted mostly of **MgUCr** and was filtered, washed with ultrapure water, and air-dried.

Structure Determination. For each of the four samples, a suitable crystal was mounted on a Bruker PLATFORM three-circle X-ray diffractometer operated at 50 keV and 40 mA and equipped with a 4K APEX CCD detector and a crystal to detector distance of ~4.7 cm. Data were collected at room temperature using graphite-monochromatized Mo Kα X-radiation and frame widths of 0.3° in ω. Comparison of the intensities of equivalent reflections measured at different times during data collection showed no significant decay for any of the four compounds. Selected data collection parameters and crystallographic data are provided in Table 1. SMART[48] software was used for data collection and SAINT[49] for data integration. Corrections for absorption were made with the programs SADABS (G. Sheldrick, unpublished) and XPREP.[50] Scattering curves for neutral atoms, together with anomalous dispersion corrections, were taken from the *International Tables for X-ray Crystallography, Volume IV*.[51] The structures were solved by direct methods and refined by full-matrix least-squares techniques on the basis of F^2 using SHELXTL.[52] Detailed crystallographic data including complete collection procedures, atomic coordinates, anisotropic displacement parameters, interatomic distances, and CIF files are provided as Supporting Information.

EPR Spectroscopy. Electron paramagnetic resonance spectra were acquired for a powder sample from the **KUCr** synthesis at X-band frequencies at both room temperature and liquid-nitrogen temperature using a Bruker EMX EPR spectrometer and Win-EPR software.

Magnetic Susceptibility. The magnetic response of 23.3 mg of powder from the **KUCr** synthesis (sealed in a gel-cap) was measured on a Quantum Design MPMS superconducting quantum interference device (SQUID) magnetometer over a temperature range 5−71 K at 100 G to determine the precise Néel temperature, and over a temperature range of 10−250 K at 30 000 G on two separate dates to determine the magnetic susceptibility and stability. The sample investigated showed no change in magnetic susceptibility over a 22-month period. Magnetization as a function of field, over the range $0 \leq H \leq 40\,000$ G, was measured at 10 and 30 K to check the assumed linearity of the response. The diamagnetic contribution of every ion to the molar susceptibility was corrected according to the method of Boudreaux and Mulay,[53] and a blank correction was made for the presence of the gel-cap and sample holder.

Table 2. Compounds Used for X-ray Absorption Spectroscopy

compound	formula	element of interest
boltwoodite[54]	$K_2[(UO_2)SiO_3(OH)]_2(H_2O)_3$	U
uranophane[55]	$Ca[(UO_2)SiO_3(OH)]_2(H_2O)_5$	U
uranophane-β[56]	$Ca[(UO_2)SiO_3(OH)]_2(H_2O)_5$	U
triuranyl diphosphate tetrahydrate[57]	$(UO_2)_3(PO_4)_2(H_2O)_4$	U
zippeite[58]	$K_3[(UO_2)_4(SO_4)_2O_3(OH)](H_2O)_3$	U
cesium orthochromate[59]	Cs_2CrO_4	Cr
potassium dichromate[60]	$K_2Cr_2O_7$	Cr
KUCr	$K_2[(UO_2)_2Cr_2O_8]$	U, Cr

X-ray Absorption Spectroscopy. X-ray absorption experiments were conducted on powder samples (Table 2) at room temperature on the BESSRC bending magnet beamline 12-BM-B[61] of the Advanced Photon Source (APS) at Argonne National Laboratory following safety protocols and procedures outlined by the Actinide Facility. U L_3 and Cr K edge data were collected employing a Si(111) double-crystal monochromator and a Pt mirror to remove the higher order harmonics that result from the high critical energy of the APS ring. Y

(44) Abraham, F.; Dion, C.; Saadi, M. *J. Mater. Chem.* **1993**, *3*, 459−463.
(45) Tabuteau, A.; Yang, H. X.; Jove, J.; Thevenin, T.; Pages, M. *Mater. Res. Bull.* **1985**, *20*, 595−600.
(46) Dickens, P. G.; Stuttard, G. P.; Ball, R. G. J.; Powell, A. V.; Hull, S.; Patat, S. *J. Mater. Chem.* **1992**, *2*, 161−166.
(47) Borène, J.; Cesbron, F. *Bull. Soc. Fr. Mineral. Cristallogr.* **1970**, *93*, 426−432.
(48) *SMART*; Bruker AXS, Madison, WI, 1998.
(49) *SAINT*; Bruker AXS, Madison, WI, 1998.
(50) *XPREP*; Bruker AXS, Madison, WI, 1998.
(51) Ibers, J. A., Hamilton, W. C., Eds.; *International Tables for X-ray Crystallography IV*; Kynoch Press: Birmingham, UK, 1974.
(52) Sheldrick, G. M. *SHELXTL NT;* version 5.1, Bruker AXS, Madison, WI, 1998.
(53) Boudreaux, E. A.; Mulay, L. N. *Theory and Applications of Molecular Paramagnetism*; John Wiley & Sons: New York, 1976; pp 494−495.
(54) Burns, P. C. *Can. Mineral.* **1998**, *36*, 1069−1075.
(55) Ginderow, D. *Acta Crystallogr.* **1988**, *C44*, 421−424.
(56) Stohl, F. V.; Smith, D. K. *Am. Mineral.* **1981**, *66*, 610−625.
(57) Locock, A. J.; Burns, P. C. *J. Solid State Chem.* **2002**, *163*, 275−280.
(58) Burns, P. C.; Deely, K. M.; Hayden, L. A. *Can. Mineral.* **2003**, *41*, 687−706.
(59) Morris, A. J.; Kennard, C. H. L.; Moore, F. H.; Smith, G.; Montgomery, H. *Cryst. Struct. Commun.* **1981**, *10*, 529−532.
(60) Brunton, G. *Mater. Res. Bull.* **1973**, *8*, 271−274.
(61) Beno, M. A.; Engbretson, M.; Jennings, G.; Knapp, G. S.; Linton, J.; Kurtz, C.; Rütt, U.; Montano, P. A. *Nucl. Instrum. Methods Phys. Res., Sect. A* **2001**, *467−468*, 699−702.

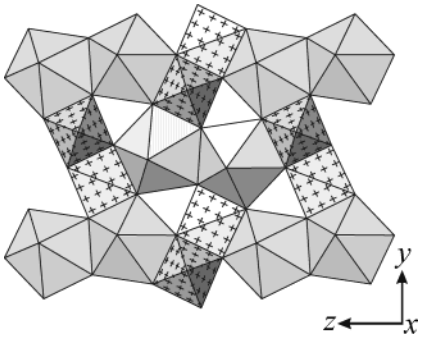

Figure 1. Structure of **KUCr** showing the sheet of uranyl UO_7 pentagonal bipyramid dimers (shaded) and chromium(V) CrO_5 square pyramid dimers (stippled) projected along [100].

and Cr metal foils were used to calibrate the beam energies at 17.038 and 5.989 keV, respectively.[62] Data were collected in the fluorescence mode, using a Lytle detector,[63] and in the transmission mode simultaneously. $\ln(I_o/I_t)$ and I_o/I_t were used for normalization of transmitted and fluorescence intensities, respectively. The data analysis methodology is described elsewhere.[64] WINXAS data analysis software[65] was used to fit the extended X-ray absorption fine structure (EXAFS) data. FEFF8.01 software[66] was used to obtain the phase and amplitude functions required for EXAFS refinement.

Results and Discussion

Structure. In all four of the uranyl chromium oxides investigated, U occurs in edge-sharing dimers of UO_7 uranyl pentagonal bipyramids, and Cr occurs as edge-sharing dimers of CrO_5 square pyramids. The two sets of dimers share edges, forming sheets of composition $[(UO_2)_2Cr_2O_8]^{2-}$, (Figure 1), which are topologically identical to uranyl divanadate sheets, $[(UO_2)_2V_2O_8]^{2-}$, of compounds of the carnotite group. **KUCr**, **RbUCr**, and **CsUCr** are isostructural with each other and with their vanadium analogues of the carnotite structural group, e.g. $K_2[(UO_2)_2V_2O_8]$;[44−46] the alkali metal cations in these compounds are located in the interlayer in 11-fold coordination by oxygen. The interatomic distances for **KUCr** and its vanadate analogue are compared in Table 3 and, on average, are identical within propagated experimental uncertainty. **MgUCr** is isostructural with its nickel uranyl vanadate analogue, $Ni[(UO_2)_2V_2O_8](H_2O)_4$;[47] in these compounds the divalent interlayer cation is coordinated by four water molecules and two uranyl ion oxygen atoms. The carnotite group is defined by its sheet anion topology,[17,18] in which edge-sharing dimers of actinyl (UO_2^{2+}, NpO_2^{2+}, NpO_2^{+}) pentagonal bipyramids share corners to form squares and triangles; the triangles remain empty, whereas the squares are populated by transition metals (V^{5+}, Nb^{5+}, Mo^{6+}) in square-pyramidal coordination. Low-valence cations and

Table 3. Selected Interatomic Distances (Å) for $K_2[(UO_2)_2(Cr_2O_8)]$[a] and $K_2[(UO_2)_2(V_2O_8)]$[44 b,c]

U(1)−O(3)	1.800(3)	U(1)−O(5)	1.797(8)
U(1)−O(5)	1.803(3)	U(1)−O(3)	1.803(8)
U(1)−O(4)#1	2.304(3)	U(1)−O(6)ii	2.308(8)
U(1)−O(4)	2.329(2)	U(1)−O(1)i	2.330(7)
U(1)−O(2)	2.345(2)	U(1)−O(4)iii	2.354(8)
U(1)−O(2)#2	2.346(2)	U(1)−O(1)	2.355(8)
U(1)−O(1)#3	2.350(2)	U(1)−O(4)	2.366(7)
⟨U(1)−O_{ap}⟩	1.802(4)	⟨U(1)−O_{ap}⟩	1.800(11)
⟨U(1)−O_{eq}⟩	2.335(5)	⟨U(1)−O_{eq}⟩	2.343(17)
Cr(1)−O(6)	1.570(3)	V(1)−O(2)	1.603(9)
Cr(1)−O(4)	1.822(3)	V(1)−O(1)	1.795(8)
Cr(1)−O(2)	1.826(2)	V(1)−O(4)	1.822(8)
Cr(1)−O(1)	1.867(3)	V(1)−O(6)	1.906(7)
Cr(1)−O(1)#4	1.899(3)	V(1)−O(6)i	1.945(8)
⟨Cr(1)−O_{eq}⟩	1.854(6)	⟨V(1)−O_{eq}⟩	1.867(16)
K(1)−O(3)	2.698(3)	K(1)−O(5)iii	2.734(9)
K(1)−O(6)#5	2.828(3)	K(1)−O(2)ii	2.800(10)
K(1)−O(3)#6	2.885(3)	K(1)−O(5)	2.882(8)
K(1)−O(1)#1	2.965(3)	K(1)−O(6)ii	2.967(8)
K(1)−O(2)#6	2.994(3)	K(1)−O(4)	2.977(7)
K(1)−O(5)#1	3.184(3)	K(1)−O(3)	3.100(10)
K(1)−O(6)#6	3.199(3)	K(1)−O(2)iii	3.181(9)
K(1)−O(5)#7	3.215(3)	K(1)−O(2)	3.253(8)
K(1)−O(5)#2	3.219(3)	K(1)−O(3)ii	3.319(9)
K(1)−O(4)#1	3.243(3)	K(1)−O(3)iii	3.372(9)
K(1)−O(6)#8	3.256(3)	K(1)−O(1)ii	3.405(7)
⟨K(1)−O⟩	3.062(10)	⟨K(1)−O⟩	3.090(29)

[a] $K_2[(UO_2)_2(Cr_2O_8)]$: a = 6.5483(8) Å, b = 8.3548(10) Å, c = 10.4200(13) Å, β = 105.040(3)°. [b] $K_2[(UO_2)_2(V_2O_8)]$: a = 6.592(5) Å, b = 8.396(4) Å, c = 10.46(1) Å, β = 104.05(7)°. [c] Symmetry transformations used to generate equivalent atoms: #1, $-x+1$, $-y$, $-z$; #2, $-x+1$, $y-1/2$, $-z+1/2$; #3, x, $-y+1/2$, $z+1/2$; #4, $-x+1$, $-y+1$, $-z$; #5, $-x+2$, $-y$, $-z$; #6, $-x+2$, $y-1/2$, $-z+1/2$; #7, $x+1$, y, z; #8, x, $y-1$, z; i, $-x$, $-y$, $-z$; ii, x, $-y+1/2$, $z+1/2$; iii, $-x$, $y+1/2$, $-z+1/2$.

H_2O groups in the interlayer region bind the sheets together. The carnotite-type sheet is chemically compliant and, combined with the wide range of possible interlayer cations, gives rise to a diverse group of minerals and synthetic compounds including sundry uranyl vanadates,[44−47,67−76] uranyl niobates,[77] neptunyl(VI) vanadates,[45] and neptunyl(V) molybdates.[78] Note that silicocarnotite is a structurally unrelated calcium silicate−phosphate.[79]

In solid oxides, chromate(V) often behaves in an essentially identical manner to vanadate(V). Both lanthanide chromates(V), $LnCrO_4$,[9−12] and lanthanide vanadates, $LnVO_4$,[80] can adopt the zircon structure, and

(62) Williams, G. P. *Electron Binding Energies*; X-ray Data Booklet, 2nd ed.; Thompson, A. C., Vaughan, D., Eds.; Lawrence Berkeley National Laboratory 2001; pp 1-1 to 1-7.
(63) Lytle, F. W.; Greegor, R. B.; Sandstrom, D. R.; Marques, E. C.; Wong, J.; Spiro, C. L.; Huffman, G. P.; Huggins, F. E. *Nucl. Instrum. Methods Phys. Res.* **1984**, *236*, 542−548.
(64) Lytle, F. W. *Experimental X-ray absorption spectroscopy*; *Applications of Synchrotron Radiation*; Winick, H., Xian, D., Ye, M. H., Huang, T., Eds.; Gordon and Breach: New York, 1989; Vol. 4, pp 135−224.
(65) Ressler, T. *J. Synchrotron Radiat.* **1998**, *5*, 118−122.
(66) Rehr, J.; de Leon, J. M.; Zabinsky, S. I.; Albers, R. C. *J. Am. Chem. Soc.* **1991**, *113*, 5135−5140.
(67) Abraham, F.; Dion, C.; Tancret, N.; Saadi, M. *Adv. Mater. Res. (Zug, Switz.)* **1994**, *1−2*, 511−520.
(68) Mereiter, K. *Neues Jahrb. Mineral., Monatsh.* **1986**, 552−560.
(69) Wenrich, K. J.; Modreski, P. J.; Zielinski, R. A.; Seeley, J. L. *Am. Mineral.* **1982**, *67*, 1273−1289.
(70) Piret, P.; DeClercq, J.-P.; Wauters-Stoop, D. *Bull. Minéral.* **1980**, *103*, 176−178.
(71) Botto, I. L.; Baran, E. J. *Z. Anorg. Allg. Chem.* **1976**, *426*, 321−332.
(72) Alekseeva, M. A.; Chernikov, A. A.; Shashkin, D. P.; Kon'kova, E. A.; Gavrilova, I. N. *Zap. Vses. Mineral. O-va.* **1975**, *103*, 576−580.
(73) Cesbron, F. *Bull. Soc. Fr. Minéral. Cristallogr.* **1970**, *93*, 320−327.
(74) Appleman, D. E.; Evans, H. T., Jr. *Am. Mineral.* **1965**, *50*, 825−842.
(75) Barton, P. B., Jr. *Am. Mineral.* **1958**, *43*, 799−817.
(76) Gaines, R. V.; Skinner, H. C. W.; Foord, E. E.; Mason, B.; Rosenzweig, A. *Dana's New Mineralogy*; John Wiley & Sons: New York, 1997; pp 779−784.
(77) Gasperin, M. *Acta Crystallogr.* **1987**, *C43*, 404−406.
(78) Grigor'ev, M. S.; Baturin, N. A.; Plotnikova, T. E.; Fedoseev, A. M.; Budantseva, N. A. *Radiochemistry (Transl. Radiokhimiya)* **1995**, *37*, 15−18.
(79) Dickens, B.; Brown, W. E. *Tschermaks Mineral. Petrogr. Mitt.* **1971**, *16*, 1−27.

Table 4. Bond Valence Sums Calculated with Different Literature Parameters for Cr

	bond valence sum or range				parameter		
	KUCr	RbUCr	CsUCr	MgUCr	*R*o	B	ref
U	6.06	6.14	6.14	6.18	2.045	0.51	83
Cr	5.25	5.18	5.10	5.41	1.794	0.37	84
O	1.77−2.23	1.85−2.22	1.90−2.28	1.63−2.21			84
Cr	4.82	4.75	4.68	4.96	1.762	0.37	85
O	1.77−2.10	1.85−2.09	1.90−2.14	1.63−2.07			85
H_2O				0.34−0.38			84
K	1.02				2.132	0.37	84
Rb		1.10			2.263	0.37	84
Cs			1.20		2.417	0.37	84
Mg				2.19	1.693	0.37	84

both of these complex ions may be found in apatite-structure materials, e.g., $Sr_5(CrO_4)_3Cl$,[81] and vanadinite, $Pb_5(VO_4)_3Cl$.[82] Square pyramidal coordination of chromium(V) by oxygen has been described from solution complexes,[2−8,13] including edge-sharing dimers of square bipyramids,[7] but does not appear to have been previously recognized in inorganic oxides. The extension of the Cr^{5+}−V^{5+} analogy from isolated tetrahedra to square pyramidal dimers raises the intriguing prospect of further similarities; vanadium(V) forms a wide variety of complex ions, including the highly polymerized decavanadate ion, $V_{10}O_{28}$,$^{6-}$ and it is possible that chromium(V) may mimic this behavior, both in solution and the solid state.

Bond Valence. The stoichiometries and structures of **KUCr**, **RbUCr**, **CsUCr**, and **MgUCr** imply that Cr is present as chromium(V). Bond valence analyses were performed using the parameters of Burns et al.[83] for $^{[7]}U^{6+}$ and Brown and Altermatt[84] for K, Rb, Cs, Mg, and Cr; for comparison, the recent parameters of Wood et al.[85] for Cr were also used. The bond valence sums are listed in Table 4; the results are consistent with Cr^{5+} and the expected oxidation states, U^{6+}, K^+, Rb^+, Cs^+, and Mg^{2+}. Interestingly, the use of bond valence parameters specific to differing Cr oxidation states makes little difference to the results for these four compounds. The sums for Cr are slightly high using the Cr^{6+} parameters of Brown and Altermatt[84] and slightly low using the Cr^{5+} parameters of Wood et al.[85] Nearly ideal results can be achieved for Cr in these four structures simply using the mean of these literature parameters, $R_o = 1.778$.

Magnetism. To confirm independently the presence of the d^1 cation Cr^{5+}, both EPR and magnetic measurements were carried out for material from the **KUCr** synthesis. The EPR spectra at room temperature and liquid-nitrogen temperature consisted of a broad unresolved signal, yielding $\langle g \rangle = 1.9802$ at room temperature, consistent with the presence of paramagnetic ions in the sample; the theoretical d^1 spin-only value is $\langle g \rangle = 2.0023$.

Figure 2 shows the variation of magnetic susceptibility as a function of temperature (χ^{-1} versus temperature is also shown). The magnetic susceptibility data are consistent with Curie−Weiss behavior and show a sharp paramagnetic−antiferromagnetic transition at the Néel temperature, $T_N = 18.5$ K. Linear regression analysis carried out on the inverse susceptibility data over the range 30−250 K yielded an effective magnetic moment higher than the expected spin-only value for a d^1 cation $= 1.732\ \mu_B$, implying the presence of an additional paramagnetic phase as an impurity.

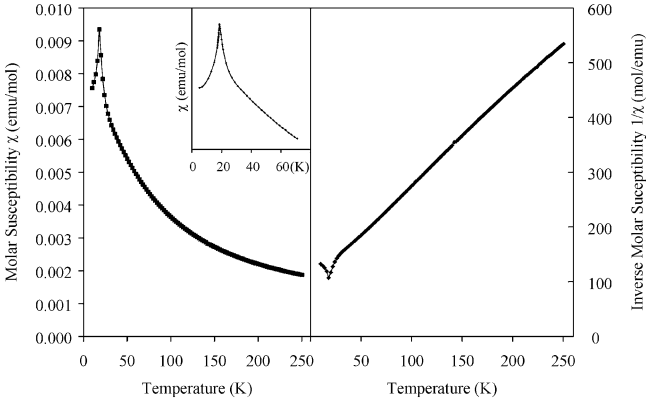

Figure 2. (Left) Temperature-dependent magnetic susceptibility of **KUCr**. The more closely spaced data of the inset reveal the Néel temperature of the antiferromagnetic transition to be 18.5 K. (Right) Inverse molar susceptibility of **KUCr**.

Rietveld analysis of powder neutron diffraction data collected at the Intense Pulsed Neutron Source from the products of a separate larger synthesis of **KUCr** revealed that sample to consist of 94.0 wt % **KUCr** and 6.0 wt % α-CrOOH (Li, unpublished results). Magnetic susceptibility data were collected (at the Chemistry Division of Argonne National Laboratory) for the sample used in the neutron diffraction studies (Skanthakumar, unpublished results) and analyzed as a two-component mixture. The effective moment of a two-component mixture is a function of the molar proportions of the phases and the squares of their moments: $(\mu_{eff})^2 =$ fraction(**KUCr**) $\times$ $(1.732\ \mu_B)^2$ + fraction(CrOOH) $\times$ $(3.873\ \mu_B)^2$. The spin-only moments for a d^1 and a d^3 system are chosen for verification of this procedure. Any unquenched orbital contribution on either Cr species will lower the observed moment, because the orbital and spin moments are opposing for less-than-half-filled d shells. An iterative refinement of these susceptibility data was performed on this two-component mixture of **KUCr** and α-CrOOH, with the mean molar mass and correction for diamagnetic susceptibilities scaled for the molar proportions of the mixture. The difference between the theoretical effective magnetic moment of the mixture and that derived from regression of the inverse susceptibility data was minimized and yielded phase proportions for **KUCr** and α-CrOOH in complete agreement with the Rietveld refinement. This result verifies the assumption of spin-only values for Cr^{3+} in α-CrOOH and Cr^{5+} in **KUCr**. Using the same iterative procedure to determine the proportions of **KUCr** and α-CrOOH in the synthesis products discussed herein yielded $\mu_{eff} = 2.13(5)\ \mu_B$, consistent with 97.2 wt % **KUCr** and 2.8(5) wt % α-CrOOH. Thus, the magnetic susceptibility data confirm the presence of Cr^{5+}, which was determined from the analysis of single-crystal X-ray data.

(80) Chakoumakos, B. C.; Abraham, M. M.; Boatner, L. A. *J. Solid State Chem.* **1994**, *109*, 197−202.
(81) Herdtweck, E. *Acta Crystallogr.* **1991**, *C47*, 1711−1712.
(82) Dai, Y.; Hughes, J. M. *Can. Mineral.* **1989**, *27*, 189−192.
(83) Burns, P. C.; Ewing, R. C.; Hawthorne, F. C. *Can. Mineral.* **1997**, *35*, 1551−1570.
(84) Brown, I. D.; Altermatt, D. *Acta Crystallogr.* **1985**, *B41*, 244.247.
(85) Wood, R. M.; Abboud, K. A.; Palenik, R. C.; Palenik, G. J. *Inorg. Chem.* **2000**, *39*, 2065−2068.

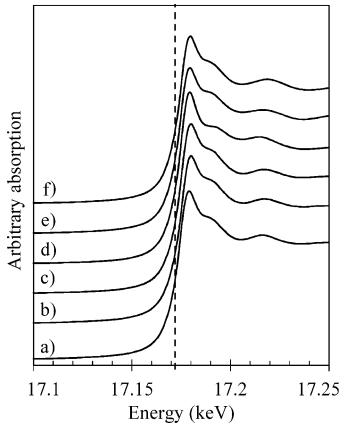

Figure 3. Uranium L_3 edge XANES of $^{[7]}U^{6+}$ in (a) boltwoodite, (b) uranophane, (c) uranophane-β, (d) triuranyl diphosphate tetrahydrate, (e) zippeite, and (f) **KUCr**. The absorption edge is indicated by the dashed line at 17.173 keV.

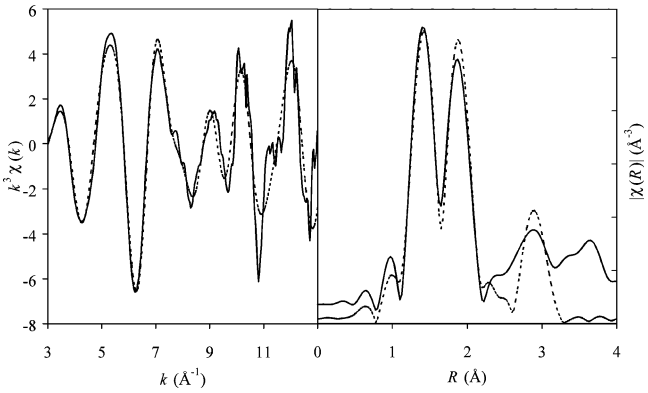

Figure 4. (Left) The k^3-weighted EXAFS of U from experiment (solid line) compared with the fit (dotted line). (Right) The magnitude of the Fourier transform of the data shown at left, uncorrected for phase shift.

X-ray Absorption Spectra. The U L_3 edge X-ray absorption near-edge structure (XANES) transmission spectra obtained from **KUCr** and the uranyl standards (Table 2) are shown in Figure 3. In all of these uranyl standards, hexavalent U occurs in 7-fold coordination, as an approximately linear $(UO_2)^{2+}$ cation coordinated by five additional ligands arranged at the equatorial positions of pentagonal bipyramids, with the uranyl O atoms at the apexes of the bipyramids. The hexavalent state of U in **KUCr** is corroborated by the very close resemblance of its XANES spectrum with those of the uranyl(VI) standards.

The k^3-weighted U L_3 EXAFS data collected from **KUCr**, together with the magnitude of their Fourier transform, are shown in Figure 4. Fitting of the U EXAFS data to a radial distance of 3.5 Å yielded results that are in excellent agreement with the structural parameters obtained from single-crystal structure refinement (Table 5), substantiating the pentagonal bipyramidal coordination of the U position in the bulk material. The U EXAFS data are not affected by the presence of the α-CrOOH impurity, as this phase does not contain any U, and thus does not contribute to the observed signal.

The Cr *K* edge XANES fluorescence spectra obtained from **KUCr** and the chromium standards (Table 2) are shown in Figure 5, along with their local coordination polyhedra. In Cs_2CrO_4, chromium occurs as the isolated

Table 5. Comparison of Structural Parameters Obtained from Single-Crystal Structure Refinement (SREF) with Those Obtained by Curve-Fitting of the U L_3 EXAFS Data

shell about uranium	method	coordination N^a	radial distance R (Å)	σ^2
O_{ap}	SREF	2	1.802(4)	
	EXAFS	1.8	1.79	0.0015
O_{eq}	SREF	5	2.335(5)	
	EXAFS	5.3	2.31	0.0038
Cr	SREF	2	3.321(1)	
	EXAFS	2.1	3.32	0.0057

[a] Precision of EXAFS results for N is usually considered ±25%.

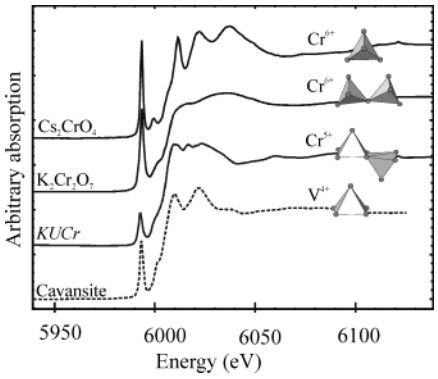

Figure 5. Coordination polyhedra and K-edge XANES spectra for Cr model compounds and **KUCr** and for V in cavansite.[88] For the purposes of comparison, the cavansite spectrum has been shifted up in energy by 524 eV.

chromate(VI) anion, CrO_4^{2-}, whereas in $K_2Cr_2O_7$, chromium is present as a dimer of corner-sharing tetrahedra, $Cr_2O_7^{2-}$. The spectra of both of these standard compounds show intense pre-edge peaks, at 5993.5 eV for Cs_2CrO_4 (fwhm 1.6 eV) and at 5993.7 eV for $K_2Cr_2O_7$ (fwhm 2.0 eV), that are attributed to electronic transitions from core states to empty bound states (1s → 3d), resulting from d^0 Cr^{6+} being present in a noncentrosymmetric site (tetrahedron).[86] The pre-edge peak is not present in chromium(III) compounds, as Cr^{3+} is generally present in regular or near-regular octahedral coordination and such electronic transitions are forbidden in centrosymmetric sites.

A less-intense pre-edge peak is also present for **KUCr** at 5992.9 eV (fwhm 2.0 eV). The d^1 nature of Cr^{5+} in **KUCr** results in lower intensity of the pre-edge peak, because fewer empty d orbitals are involved in the 1s → 3d transitions.[87] This effect is also observed in the rather similar V K edge XANES spectrum (Figure 5) of the mineral cavansite,[88] $Ca[(VO)Si_4O_{10}](H_2O)_4$, in which V also occurs in square pyramidal coordination as a d^1 cation, V^{4+}. Note that for the purposes of comparison, the cavansite V *K* edge spectrum in Figure 5 has been shifted up in energy by 524 eV. The presence of the minor α-CrOOH impurity (2.8 wt %) also tends to decrease the intensity of the pre-edge peak of the **KUCr** sample, albeit only by a slight amount.

Chromate(VI) Analysis by XANES. The very soluble chromate(VI) ion is both toxic and carcinogenic, result-

(86) Hanson, A. L.; Bajt, S.*Philos. Mag. B* **1997**, *75*, 909−924.
(87) Jousseaume, C.; Ribot, F.; Kahn-Harari, A.; Vivien, D.; Villain, F. *Nucl. Instrum. Methods Phys. Res., Sect. B* **2003**, *200*, 425−431.
(88) Locock, A.; Luth, R. W.; Cavell, R. G.; Smith, D. G. W.; Duke, M. J. M. *Am. Mineral.* **1995**, 80, 27−38.

ing in chromium(VI) being ranked 18 of 275 on the CERCLA List of Priority Hazardous Substances.[89] XANES has been widely applied to the quantitative analysis of chromate(VI) in environmental and industrial samples.[90−97] This technique is based on the magnitude of the pre-edge peak that is present for chromium(VI), and absent for chromium(III), the two most common stable oxidation states of chromium. The presence of a less-intense pre-edge peak due solely to Cr^{5+} in the XANES spectrum of **KUCr** sounds a cautionary note for such two-component determination of chromate(VI) content. The **KUCr** pre-edge peak overlaps with those of the chromate(VI) standards, implying that a mixture of Cr^{6+} and Cr^{5+} would be indistinguishable (by XANES spectroscopy) from a mixture (albeit in differing proportion) of Cr^{6+} and Cr^{3+}, as the presence of Cr^{5+} and Cr^{3+} both serve to attenuate the pre-edge signal of the Cr^{6+}.

Although chromium(V) is not generally considered to be a stable oxidation state in the environment, the synthesis under mild hydrothermal conditions of stable **KUCr** and its related carnotite-type compounds imply that such phases may exist under certain geological conditions. The geochemical cycle of chromium only rarely interacts with that of uranium, although the mineral rilandite, $(Cr^{3+},Al)_6SiO_{11}(H_2O)_5$, was described as occurring with carnotite, $K_2[(UO_2)_2V_2O_8](H_2O)_n$, in uranium deposits of the Colorado Plateau.[98] However, chromium(VI) is a common contaminant, along with uranium(VI), at the Hanford, WA site, resulting from decades of U.S. nuclear production. XANES spectroscopy has been used to study the speciation of both Cr and U in Hanford sediments, and the chromate(VI) content was determined through analysis of the pre-edge peak.[99] It is probable that chromium(V) is also present in the Hanford subsurface for some time period; synchrotron-based FTIR investigation of biogeochemical reduction of chromium(VI) in basalt samples from the similarly contaminated Idaho National Engineering and Environmental Laboratory site showed that chromium(V) intermediates persist for more than 2 weeks.[100] The possibility that uranium may stabilize chromium(V) in **KUCr**-like compounds in the subsurface at Hanford requires investigation and suggests that determination of chromate(VI) content by XANES spectroscopy may not be straightforward. Both Raman and FTIR spectroscopies show unique modes for chromate(V) and chromate(VI),[11,100] and these techniques could be used to complement and verify XANES results.

Acknowledgment. We thank R.G. Hayes for the acquisition of the EPR spectra, I. Todorov and F. Gascoin for assistance with the magnetic susceptibility measurements, and S. Sevov for helpful discussions. We thank Y. Li for the neutron diffraction results. We are grateful to S. Krivovichev for encouraging this work. A.J.L. thanks the Environmental Molecular Sciences Institute, University of Notre Dame, for a 2003 EMSI Fellowship, and the International Centre for Diffraction Data, for a 2003 Ludo Frevel Crystallography Scholarship. This research was carried out with the support of the Actinide Facility of Argonne National Laboratory and the BESSRC-CAT. This research was funded by the Environmental Management Sciences Program of the United States Department of Energy (DE-FGO7-97-ER14820). The work at Argonne, including the Actinide Facility, BESSRC, and the Advanced Photon Source, was supported by the United States Department of Energy, Office of Science, Office of Basic Energy Sciences, under Contract No. W-31-109-ENG-38.

Supporting Information Available: Tables of complete collection procedures and structure refinement details, atomic coordinates, interatomic distances and angles, bond valence calculations, and crystallographic information files (CIF). This material is available free of charge via the Internet at http://pubs.acs.org.

CM030639C

(89) Agency for Toxic Substances and Disease Registry (ATSDR) *Toxicological profile for chromium*; U.S. Department of Health and Human Services, Public Health Service: Atlanta, GA, 2000.
(90) Bajt, S.; Clark, S. B.; Sutton, S. R.; Rivers, M. L.; Smith, J. V. *Anal. Chem.* **1993**, *65*, 1800−1804.
(91) Wan, J.; Thompson, G. E.; Lu, K.; Smith, C. J. E. *Physica B (Amsterdam)* **1995**, *208−209*, 511−512.
(92) Lee, J. F.; Bajt, S.; Clark, S. B.; Lamble, G. M.; Langton, C. A.; Oji, L. *Physica B (Amsterdam)* **1995**, *208−209*, 577−578.
(93) Peterson, M. L.; Brown, G. E., Jr.; Parks, G. A. *Colloids Surf., A* **1996**, *107*, 77−88.
(94) Rinehart, T. L.; Schulze, D. G.; Bricka, R. M.; Bajt, S.; Blatchley, E. R., III *J. Hazard. Mater.* **1997**, *52*, 213−221.
(95) Peterson, M. L.; White, A. F.; Brown, G. E., Jr.; Parks, G. A. *Environ. Sci. Technol.* **1997**, *31*, 1573−1576.
(96) Peterson, M. L.; Brown, G. E., Jr.; Parks, G. A.; Stein, C. L. *Geochim. Cosmochim. Acta* **1997**, *61*, 3399−3412.
(97) Huggins, F. E.; Najih, M.; Huffman, G. P. *Fuel* **1999**, *78*, 233−242.
(98) Henderson, E. P.; Hess, H. L. *Am. Mineral.* **1933**, *18*, 195−205.
(99) Catalano, J. G.; Warner, J. A.; Ainsworth, C. C.; Zachara, J. M.; Traina, S. J.; Brown, G. E., Jr. *Abs. Pap.−Am. Chem. Soc.* **2002**, *1*, GEOC-126.
(100) Holman, H.-Y. N.; Martin, M. C.; Lamble, G. M.; McKinney, W. R.; Hunter-Cevera, J. C. *Geomicrobiol. J.* **1999**, *16*, 307−324.